Supporting Information

Spin and Orbital Magnetic Moment Anisotropies of Monodispersed Bis(Phthalocyaninato)Terbium on a Copper Surface

Sebastian Stepanow,[*,⊥] Jan Honolka,[⊥] Pietro Gambardella,[#,‖] Lucia Vitali,[⊥,↕,∩] Nasiba Abdurakhmanova,[⊥] Tzu-Chun Tseng,[⊥] Stephan Rauschenbach,[⊥] Steven L. Tait,[°] Violetta Sessi,[⊥] Svetlana Klyatskaya,[§] Mario Ruben,[§,‡] and Klaus Kern[⊥,†]

[⊥]*Max-Planck-Institut für Festkörperforschung, Heisenbergstrasse 1, D-70569 Stuttgart, Germany,*

[#]*Centre d'Investigació en Nanociència i Nanotecnologia (ICN-CSIC), UAB Campus, E-08193 Barcelona, Spain,*

[‖]*Institució Catalana de Recerca i Estudis Avançats (ICREA), E-08100 Barcelona, Spain,*

[↕] *IKERBASQUE, Basque Foundation for Science, E-48011, Bilbao, Spain*

[∩]*Centro de Fisica de Materiales CFM-MPC, Centro Mixto CSIC-UPV, E-20018 San Sebastian, Spain*

[°]*Department of Chemistry, Indiana University, Bloomington, IN 47405,USA,*

[§]*Institute of Nanotechnology, Karlsruhe Institute of Technology (KIT), D-76344 Eggenstein-Leopoldshafen, Germany,*

[‡]*IPCMS-CNRS UMR 7504, Université de Strasbourg, 23 Rue du Loess, F-67034 Strasbourg, France, and*

[†]*Institut de Physique de la Matière Condensée, Ecole Polytechnique Fédérale de Lausanne, CH-1015 Lausanne, Switzerland*

*Email: s.stepanow@fkf.mpg.de

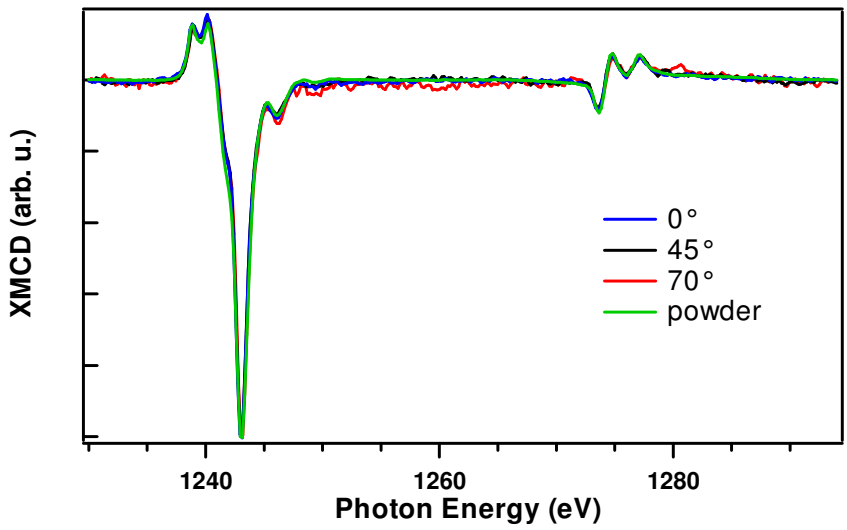

Figure S1: Comparison of XMCD data for $TbPc_2$ on Cu(100) and powder sample normalized to the same M_5 intensity.

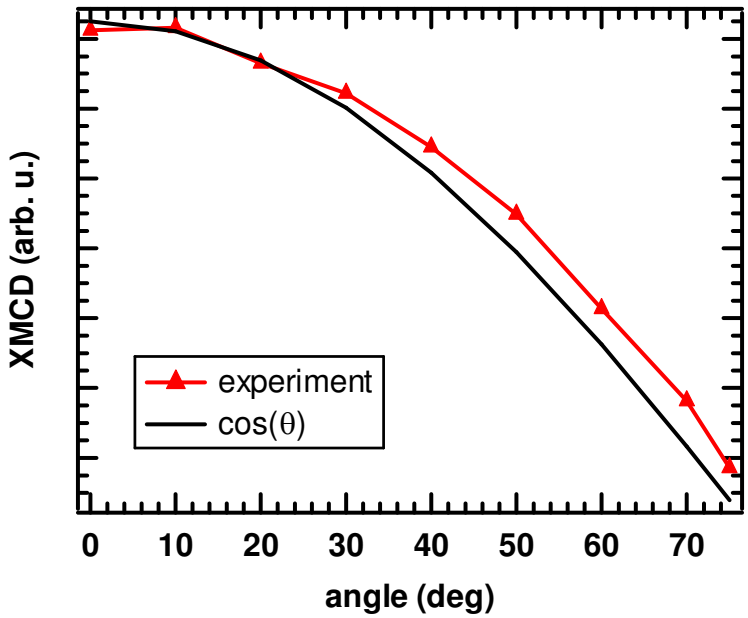

Figure S2. Angular dependence of the M_5 XMCD of $TbPc_2$ on Cu(100) (T = 8 K, B = 5 T). A cosine function of the angle is plotted as well, which is expected for a moment fully polarized out-of-plane.

Synthesis

The synthesis was obtained by using several modifications of the protocol based on the published procedure reported.[1] The synthesis was accomplished by templating reactions, starting from a mixture of the phthalonitrile precursor o-dicyanobenzene and the terbium acetylacetinate $Tb(acac)_3$ nH_2O, in the presence of a strong base (DBU) and high-boiling solvents, such as pentanol or hexanol, following the published route[1] with some modifications detailed below.

A mixture of 1,2-dicyanobenzene (42 mmol), $Tb(acac)_3{\cdot}4H_2O$ (5 mmol), and 1,8-diazabicyclo[5.4.0]undec-7-ene (DBU) (21 mmol) in 50 mL of 1-pentanol was refluxed for 1.5 d. The solution was allowed to cool to room temperature and then acetic acid was added and mixture was heated at 100 °C for 0.5h. The precipitate was collected by filtration and washed with *n*-hexane and Et_2O. The crude purple product was redissolved in 800 ml of $CHCl_3$/MeOH (1/1) and undissolved PcH_2 was filtered off. Both forms, blue (anionic $[TbPc_2]^-$) and green (neutral $[TbPc_2]^0$), were obtained simultaneously, as revealed by electronic absorption spectra.[1] In order to convert the unstabilized anionic form to the neutral one, the reaction mixture was presorbed on active (0 % H_2O) basic alumina oxide. Purification was carried out by column chromatography on basic alumina oxide (deactivated with 4.6 % H_2O, level IV) with chloroform/methanol mixture (10:1) as an eluent. Analytically pure powder samples were achieved in this way with 30 % yield.

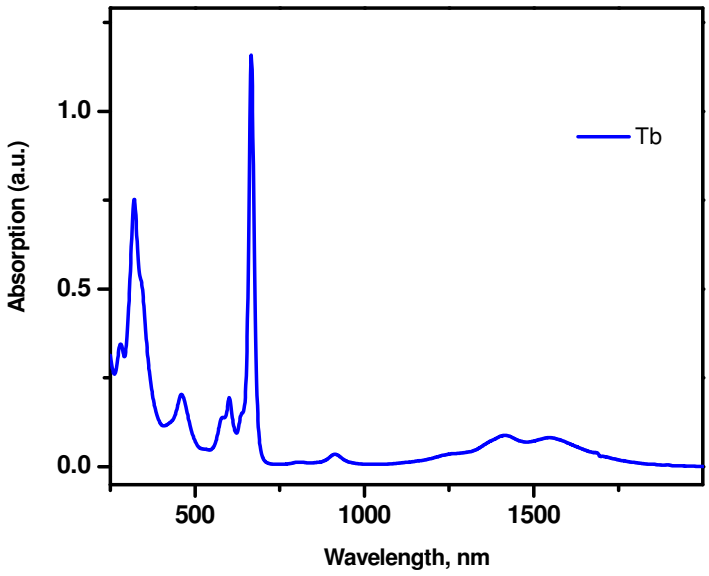

Figure S3. UV-Vis-near IR spectrum of **[TbPc$_2$]^0** in $CHCl_3$.

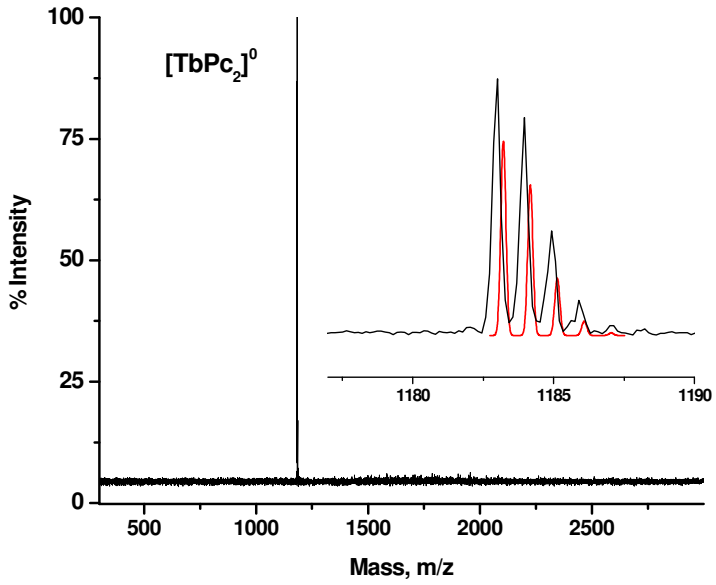

Figure S4. MALDI-ToF spectra of the complex **[TbPc$_2$]^0**

Integrity of thermally evaporated $TbPc_2$ molecules on metal surfaces

The structural conformation of single molecule magnets is a crucial point for their magnetic properties. Grafting and deposition of SMMs on surfaces can result in decomposition or conformational changes of the molecules that ultimately destroy their extraordinary magnetic behavior. To check the thermal stability of $TbPc_2$ and its integrity on the surface we carried out electrospray time-of-flight mass spectrometry (ES-TOF-MS) of the powder material before and after sublimation. Furthermore, we analyzed the evaporated material recovered by washing off a thin film of $TbPc_2$ prepared at different sublimation temperatures in ultra-high vacuum. In addition, a series of STM measurements on the self-assembly of $TbPc_2$ on Cu(100), Cu(111) and Au(111) surfaces proves the purity of the $TbPc_2$ layers at the molecular level.[2]

For the ES-MS measurements the molecules were dissolved in dichlormethane (DCM). Sublimated molecules were recovered by casting droplets of 10 µl DCM onto the substrates and picking them up with a pipette seconds later. The solutions were further diluted 1:2 with ethanol and electrosprayed in positive mode from an offline nanospray source. Figure S5 shows the mass spectra of the dissolved pristine powder (reference) as well as of the recovered material from the substrate after evaporation at 652 K and 822 K. In all three spectra the base peak is found at 1183 Th corresponding to $TbPc_2^+$, showing that intact molecules can be evaporated and deposited in vacuum. After evaporation at higher temperatures also $Tb_2Pc_3^+$ and $Tb_2Pc_4^+$ clusters can be detected. This finding indicates an onset of thermal decomposition. However, the observation of the larger clusters could be due to the recombination of fragments in the solution from single Pcs and TbPc. Similar mass spectra are found for the material remaining in the crucible at the respective temperature. Other contaminations, in particular in the low m/z range, could not be attributed to the $TbPc_2$ sample. Note that nanospray mass spectrometry is sensitive to tiny amounts of material, which is also valid for any kind of contamination.

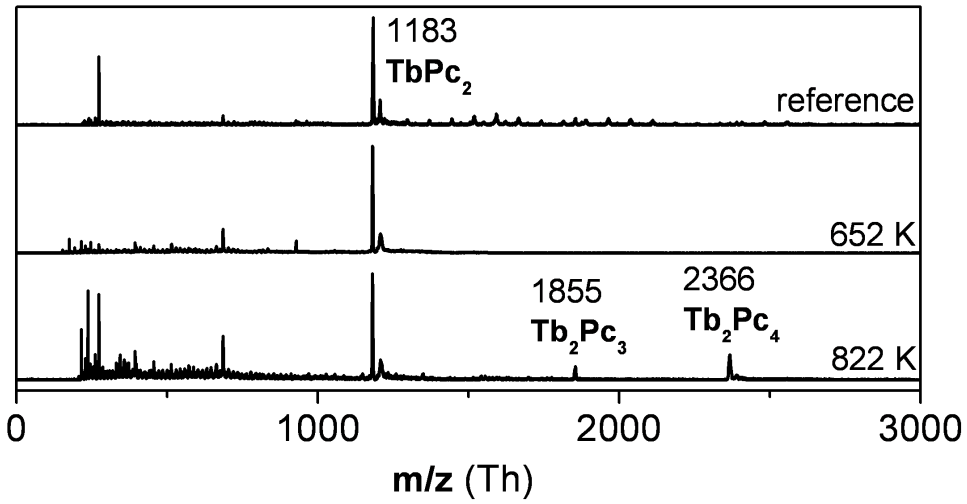

Figure S5. Electrospray ionization time-of-flight mass spectra of $TbPc_2$. The pristine powder dissolved in dichlormethane and ethanol served as a reference for comparison. After the evaporation $TbPc_2$ (1183 Th) is recovered from the surface. Moreover at high sublimation temperatures larger Tb_xPc_y clusters are found.

The electrospray mass spectrometry data shows that $TbPc_2$ has an extraordinary high thermal stability, and can be evaporated and deposited without decomposition. However, mass spectrometry cannot prove that exclusively intact $TbPc_2$ are deposited onto the surface. In order to ensure the purity and integrity of our molecular films, we performed extensive scanning tunneling microscopy studies on gold and copper surfaces. Figure S6 shows a Cu(100) surface at room temperature after the evaporation of a small amount of $TbPc_2$. Two species of molecules can be identified, $TbPc_2$ with a height of 430 pm and Pc (or TbPc) with a height of 160 pm. These values are comparable to the findings for $TbPc_2$ deposition on Au(111) in Ref. 3. After careful degassing of the $TbPc_2$ powder, only a single species of 430 pm height is observed whose appearance is nearly identical on the different metal surfaces. Thus we conclude that pure $TbPc_2$ films can be achieved.

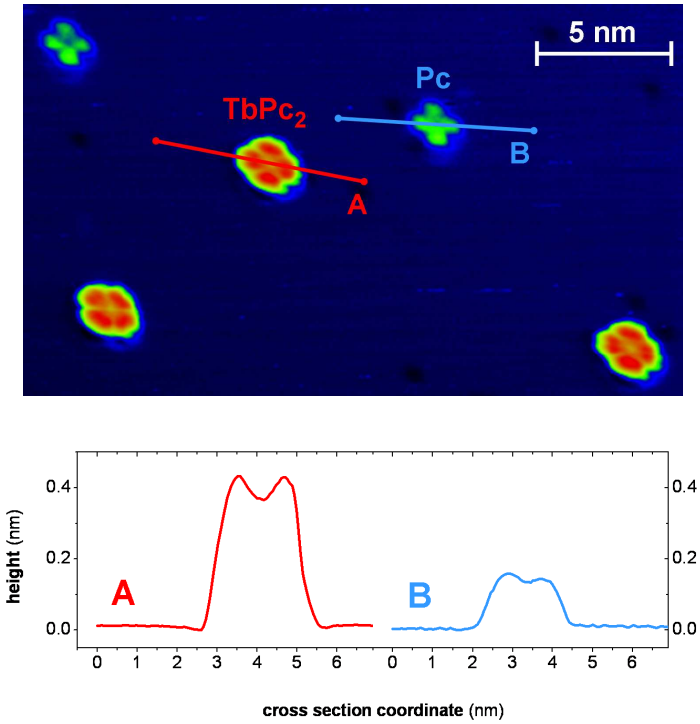

Figure S6. STM topograph and line profiles of $TbPc_2$ and Pc on Cu(100) measured at room temperature.

XAS simulations for free Tb(III) ion

Following reference 4 the XAS spectra for linear polarization with the E-vector along and perpendicular to the internal symmetry axis can be simulated with the transitions $\Delta J = 0$ and $\Delta J = \pm 1$, respectively. The spectra were calculated using the TT MULTIPLET code (Slater-Condon parameter scaling: 80% of their Hartree-Fock value, lineshape broadening: Lorentzian 0.2 eV, Gaussian 0.4 eV).

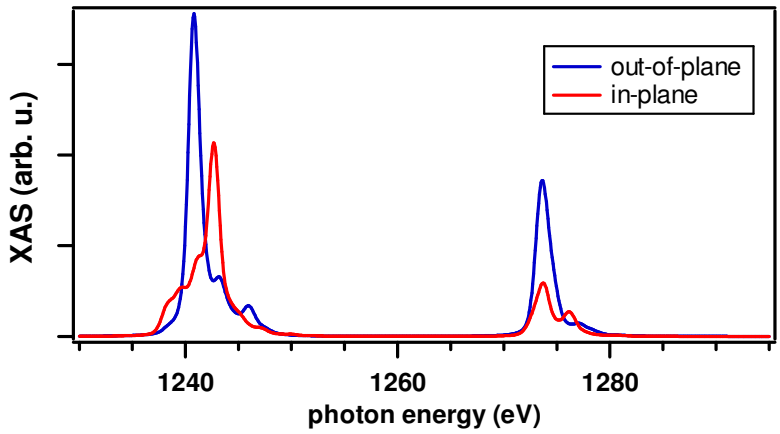

Figure S7. XAS simulation for Tb(III) for $\Delta J = 0$ (out-of-plane) and $\Delta J = \pm 1$ (in-plane) transitions.

Description of ligand field multiplet calculation

To interpret the magnetic properties of the $TbPc_2$ molecules obtained by XMCD measurements, we used ligand field multiplet theory as it allows to calculate the orbital (L_σ) and spin (S_σ and T_σ) magnetic moments separetly.[5-8] The single-ion Hamiltonian contains the usual atomic terms for the electron kinetic energy, nuclear attraction, electron repulsion, and spin-orbit coupling. The first two terms yield the average energy of the configuration. The electron-electron repulsion is treated in the Hartree-Fock approximation and expressed by the Slater-Condon-Shortley parameters (F_i and G_i). The spherical part of the electron-electron interaction is added to the average energy of the configuration. The parameters F_i and G_i and the spin-orbit coupling constants are obtained using the atomic theory code developed by Cowan.[5] In the crystal field limit, the ground state is given by a single electronic configuration f^N (where N is the number of valence f electrons), split in energy by electron repulsion and ligand field potential. The molecular environment is modeled by an electric potential that reflects the point group symmetry of the metal ion site. The many electron wavefunction of a single configuration is represented by a linear combination of determinantal product states with basis wavefunctions of the form $R_n(r)\ Y_{km}(\theta,\varphi)\ \chi(\sigma)$, which separates into the radial part $R_n(r)$, the spherical harmonics Y_{km} for the angular dependence, and the spin function $\chi(\sigma)$. The matrix elements of the radial part for the different terms of the Hamiltonian are given by the Slater-Condon-Shortley parameters and crystal field potential parameters. The non-spherical part of the total Hamiltonian is numerically diagonalized, including the Zeeman energy term,

$$H_Z = \sum_{i=1}^{N} \frac{\mu_B}{\hbar} \mathbf{B} \cdot (2\mathbf{s}^i + \mathbf{l}^i)$$

Here, $\boldsymbol{s}^i$ and $\boldsymbol{l}^i$ are the one-electron spin and orbital kinetic momentum operators that add up to give the total atomic spin ($\boldsymbol{S}$) and orbital moments ($\boldsymbol{L}$). In low-symmetry environments, the anisotropic charge distribution that results from strongly directional bonds or crystal field induces an inhomogeneous spatial distribution of the spin density over the atomic unit cell.[9] Such a spin anisotropy can be expressed as a nonzero spin dipole moment, which affects the XMCD intensity through the angular dependence of the transition matrix elements. The spin dipole momentum operator of a single electron is defined as

$$\boldsymbol{t} = \boldsymbol{s} - \frac{3\boldsymbol{r}(\boldsymbol{r}\cdot\boldsymbol{s})}{r^2}$$

For an *N*-electron atom, the intra-atomic spin dipole operator is then given as

$$\mathbf{T} = \sum_{i=1}^{N} \mathbf{t}^i$$

The expectation values of the atomic kinetic momentum operators $\boldsymbol{M} = \boldsymbol{L}$, $\boldsymbol{S}$, and $\boldsymbol{T}$ of state $|\Psi\rangle$

projected onto the direction $\boldsymbol{e}_\theta$ were calculated as

$$\begin{aligned}\langle M_\theta \rangle &= \langle \Psi | \mathbf{M}\cdot\boldsymbol{e}_\theta | \Psi \rangle \\ &= (\boldsymbol{e}_\theta\cdot\boldsymbol{e}_x)\,\langle M_x\rangle + (\boldsymbol{e}_\theta\cdot\boldsymbol{e}_y)\,\langle M_y\rangle + (\boldsymbol{e}_\theta\cdot\boldsymbol{e}_z)\,\langle M_z\rangle\end{aligned}$$

To take finite temperature effects into account, the moments were weighted by the Boltzmann

distribution according to

$$\langle M_\theta(T)\rangle = \frac{1}{Z}\sum_{\Psi}\left\langle M_\theta^{\Psi}\right\rangle e^{-\frac{E_\Psi}{k_B T}}$$

where

$$Z = \sum_{\Psi} e^{-\frac{E_\Psi}{k_B T}}$$

Note that, at the $M_{4,5}$ edge, *i.e.*, for the 3*d* to 4*f* transitions, the effective spin moment reads μ_{Sz} (eff) = μ_{Sz} + 6 T_z rather than μ_{Sz} (eff) = μ_{Sz} + 7 T_z as in the case of the $L_{2,3}$ edges of transition metals.[10]

Tb parameters

The Tb ion was represented by a f^8 configuration corresponding to an oxidation state +3. The molecular environment was modeled by a D_{4d} crystal field potential with non-zero parameters (B_{km} = $A_k^m\langle r^k\rangle$) B_{20} = 414 cm^{-1}, B_{40} = -228 cm^{-1}, and B_{60} = 33 cm^{-1} in the expansion of the crystal field potential $\boldsymbol{F}$,

$$\mathbf{F} = A_2^{\,0}\langle r^2\rangle\alpha\mathbf{O}_2^{\,0} + A_4^{\,0}\langle r^4\rangle\beta\mathbf{O}_4^{\,0} + A_4^{\,4}\langle r^4\rangle\beta\mathbf{O}_4^{\,4} + A_6^{\,0}\langle r^6\rangle\gamma\mathbf{O}_6^{\,0} + A_6^{\,4}\langle r^6\rangle\gamma\mathbf{O}_6^{\,4}$$

as reported by Ishikawa *et al*.[11] The temperature was taken from the experiment to be $T = 8$ K. The spin-orbit coupling constants for the 4*f* shells is $\lambda_{4f} = 221$ meV, and the Slater-Condon-Shortley parameters are $F_2 = 14.915$ eV, $F_4 = 9.360$ eV, and $F_6 = 6.734$ eV, all obtained using Cowan's Code within the Hartree-Fock approximation. The latter were scaled to 80% to account for the overestimation of the electron-electron repulsion in the atomic calculations. The parameters are the same used by Thole and co-workers reported in ref. 12.

Complete Ref. 1:

Gambardella, P.; Stepanow, S.; Dmitriev, A.; Honolka, J.; de Groot, F. M. F.; Lingenfelder, M.; Gupta, S. S.; Sarma, D. D.; Bencok, P.; Stanescu, S.; Clair, S.; Pons, S.; Lin, N.; Seitsonen, A. P.; Brune, H.; Barth, J. V.; Kern, K. *Nature Mater.* **2009**, *8*, 189.

References

(1) (a) Moussavi, M.; De Cian, A.; Fischer, J.; Weiss, R. *Inorg. Chem.* **1988**, *27*, 1287. (b) Koike, N.; Uekusa, H.; Ohashi, Y.; Harnoode, C.; Kitamura, F.; Ohsaka, T.; Tokuda, K. *ibid.* **1996**, *35*, 5798. (c) Kasuga, K.; Tsutsui, M.; Petterson, R. C.; Tatsumi, K.; Van Opdenbosch, N.; Pepe, G.; Meyer, E. F. *J. Am. Chem. Soc.* **1980**, *102*, 4835.

(2) Deng, Z.; Rauschenbach, S.; Stepanow, S.; Klyatskaya, S.; Ruben, M.; Kern K. *in preparation*.

(3) Katoh, K.; Yoshida, Y.; Yamashita, M.; Miyasaka, H.; Breedlove, B. K.; Kajiwara, T.; Takaishi, S.; Ishikawa, N.; Isshiki, H.; Zhang, Y. F.; Komeda, T.; Yamagishi, M.; Takeya, J. *J. Am. Chem. Soc.* **2009**, *131*, 9967.

(4) Goedkoop, J. B.; Thole, B. T.; van der Laan, G.; Sawatzky, G. A.; de Groot, F. M. F.; Fuggle, J. C. *Phys Rev. B* **1988**, *37*, 2086.

(5) R. D. Cowan, The Theory of Atomic Structure and Spectra (University of California Press, Berkeley, 1981).

(6) F. M. F. de Groot and A. Kotani, Core Level Spectroscopy of Solids (CRC Press, 2008).

(7) van der Laan, G.; Thole, B. T. *Phys. Rev. B* **1991**, *43*, 13401.

(8) Stepanow, S; Mugarza, A.; Ceballos, G.; Moras, P.; Cezar, J. C.; Carbone, C.; Gambardella, P. *Phys. Rev. B* **2010**, *82*, 014405.

(9) Stöhr, J.; König, H. *Phys. Rev. Lett.* **1995**, *75*, 3748.

(10) Thole, B. T.; Carra, P.; Sette, F.; van der Laan, G. *Phys. Rev. Lett.* **1992**, *68*, 1943.

(11) Ishikawa, N.; Sugita, M.; Okubo, T.; Tanaka, N.; Iino, T.; Kaizu, Y. *Inorg. Chem.* **2003**, *42*, 2440.

(12) Thole, B. T.; van der Laan, G.; Fuggle, J. C.; Sawatzky, G. A.; Karnatak, R. C.; Esteva, J.-M. *Phys. Rev. B* **1985**, *32*, 5107.